
This is an electronic reprint of the original article.
This reprint may differ from the original in pagination and typographic detail.

Yang, Mingze; Lenarda, Anna; Frindy, Sana; Sang, Yushuai; Oksanen, Valtteri; Bolognani, Adriano; Hendrickx, Lisa; Helaja, Juho; Li, Yongdan

A metal-free carbon catalyst for oxidative dehydrogenation of aryl cyclohexenes to produce biaryl compounds

Published in:

Proceedings of the National Academy of Sciences of the United States of America

DOI:

[10.1073/pnas.2303564120](https://doi.org/10.1073/pnas.2303564120)

Published: 24/07/2023

Document Version

Publisher's PDF, also known as Version of record

Published under the following license:

CC BY-NC-ND

Please cite the original version:

Yang, M., Lenarda, A., Frindy, S., Sang, Y., Oksanen, V., Bolognani, A., Hendrickx, L., Helaja, J., & Li, Y. (2023). A metal-free carbon catalyst for oxidative dehydrogenation of aryl cyclohexenes to produce biaryl compounds. *Proceedings of the National Academy of Sciences of the United States of America*, 120(31), e2303564120. Article e2303564120. <https://doi.org/10.1073/pnas.2303564120>

This material is protected by copyright and other intellectual property rights, and duplication or sale of all or part of any of the repository collections is not permitted, except that material may be duplicated by you for your research use or educational purposes in electronic or print form. You must obtain permission for any other use. Electronic or print copies may not be offered, whether for sale or otherwise to anyone who is not an authorised user.



A metal-free carbon catalyst for oxidative dehydrogenation of aryl cyclohexenes to produce biaryl compounds

Mingze Yang^a , Anna Lenarda^b, Sana Frindy^b, Yushuai Sang^a, Valterri Oksanen^b, Adriano Bolognani^b, Lisa Hendrickx^b, Juho Helaja^{b,1} , and Yongdan Li^{a,1}

Edited by Alexis Bell, University of California, Berkeley, CA; received March 8, 2023; accepted May 30, 2023

A metal-free route based on a carbon catalyst to synthesize biphenyls through oxidative dehydrogenation (ODH) of phenyl cyclohexene has been investigated. Among the samples examined, an air-oxidized active carbon exhibits the best activity with a $9.1 \times 10^{-2} \text{ h}^{-1}$ rate constant, yielding 74% biphenyl in 28 h at 140 °C under five bar O₂ in anisole. The apparent activation energy is measured as 54.5 kJ·mol⁻¹. The extended reaction scope, consisting of 15 differently substituted phenyl cyclohexenes, shows the wide applicability of the proposed method. The catalyst's good recyclability over six runs suggests this ODH method as a promising route to access the biaryl compounds. In addition, the reaction mechanism is investigated with a combination of X-ray photoelectron spectroscopy, functional group blocking, and model compounds of carbon catalysts and is proposed to be based on the redox cycle of the quinoidic groups on the carbon surface. Additional experiments prove that the addition of the catalytic amount of acid (methanesulfonic acid) accelerates the reaction. In addition, Hammett plot examination suggests the formation of a carbonium intermediate, and its possible structure is outlined.

biaryl synthesis | catalysis without metal | carbon | oxidative dehydrogenation | reaction mechanism

Biaryls are a common structural unit in a wide range of fine chemicals, which find application in various fields, e.g., pharmaceuticals, agrochemicals, precursors of electronic materials, and ligands to metal ions or atoms (1). This unit is also vastly present in natural products (1). According to an early 2,000s article, the biaryl structure exists in 4.3% of the known drugs, making it a crucial subunit for the pharmaceutical industry (2). At present, two are the main routes industrially employed to access biaryls: transition metal catalyzed reactions, e.g., classic Pd-catalyzed couplings, which offer reliable and convenient procedures, but make use of toxic substrates, i.e., boronic acids, and an unstable and precious catalyst, a Pd⁰ complex (3, 4), and the direct aromatization of functionalized aryl cyclohexenes via oxidative dehydrogenation (ODH) (5, 6). In this case, the substrates, aryl cyclohexenes, are commercially available and easy to prepare via Grignard reactions (7, 8), which makes this route more environmentally benign.

Traditional ODH reactions are catalyzed by various transition metal and metal oxide catalysts like nickel (9, 10), copper (11, 12), palladium (11, 13), platinum (14, 15), and vanadium oxide (16). For example, the industrial production of styrene from ethylbenzene utilizes vanadium oxide as the catalyst, while Cu⁰/Selectfluor (commercialized fluorine donor) is employed for the ODH reaction of phenyl cyclohexene (17).

Over the past decades, carbon has been developed as a metal-free and green alternative catalyst for ODH reactions (18). A wide range of carbon materials have been utilized as catalysts in ODH reactions, including both well-defined nanostructures like nanodiamonds (19), carbon nanotubes (19), graphenes, fibers (20), and amorphous activated carbons (ACs) (21). In addition, a broad range of substrates have been investigated, such as ethane (22), propane (23, 24), n-butane (25), i-butane (26), ethylbenzene (20, 27), and N-heterocyclics (28, 29). Su and his coworkers (27, 30) explored the ODH reaction of ethylbenzene to styrene with carbon nanotubes as a catalyst and proposed ketonic and quinoidic groups as the active site of carbon nanotubes in gas-phase ODH reaction. Recently, Enders et al (28) investigated the ODH reaction of N-heterocycles in the liquid phase with activated carbon as the catalyst and proposed the redox cycle of the surface quinoidic group as the active site. However, the carbon-catalyzed ODH reaction of aryl cyclohexenes in the liquid phase to access biaryls is currently limitedly investigated.

Herein, the carbon-catalyzed ODH of aryl cyclohexenes to biaryls is investigated. The activity of different AC catalysts is compared using kinetic parameters and the

Significance

Biaryls are important structural units which are fundamental in varieties of compounds. Oxidative dehydrogenation (ODH) reaction is a potential way to access biaryls from cyclic alkanes. Nowadays, carbon-based catalysts have been developed for olefins production as a catalyst of ODH reaction for much more environmentally benign production. However, metal-free carbon-based catalysts have not been fully investigated as a catalyst for the synthesis of biaryls. Herein, an air-oxidized active carbon shows high activity in the ODH reaction of phenyl cyclohexene. This work also provides a deep understanding of the active sites on active carbon and the mechanism of the phenyl cyclohexene to biaryl ODH action, which will broaden the application of carbon as metal-free catalysts in green chemical production.

Author contributions: J.H. and Y.L. designed research; M.Y., A.L., S.F., Y.S., V.O., A.B., L.H., J.H., and Y.L. performed research; A.L., S.F., V.O., A.B., L.H., and Y.L. contributed new reagents/analytic tools; M.Y., A.L., S.F., Y.S., V.O., A.B., L.H., J.H., and Y.L. analyzed data; and M.Y., A.L., Y.S., J.H., and Y.L. wrote the paper.

The authors declare no competing interest.

This article is a PNAS Direct Submission.

Copyright © 2023 the Author(s). Published by PNAS. This article is distributed under [Creative Commons Attribution-NonCommercial-NoDerivatives License 4.0 \(CC BY-NC-ND\)](https://creativecommons.org/licenses/by-nc-nd/4.0/).

¹To whom correspondence may be addressed. Email: juho.helaja@helsinki.fi or yongdan.li@aalto.fi.

This article contains supporting information online at <https://www.pnas.org/lookup/suppl/doi:10.1073/pnas.2303564120/-DCSupplemental>.

Published July 24, 2023.

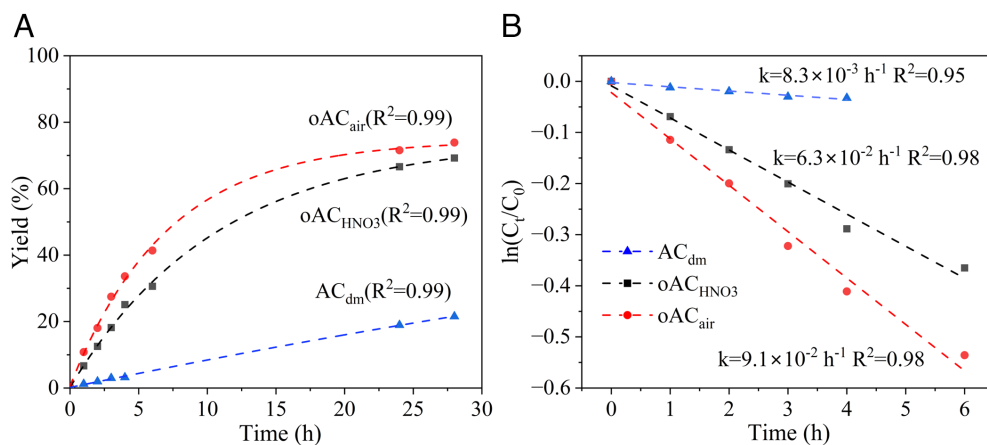


Fig. 1. (A) The yield-time curves of the ODH reaction in anisole with different catalysts under five bar O_2 at 140 °C (B) The relationship between $\ln(C_t/C_0)$ and reaction time with different catalysts.

apparent activation energy of the reaction. In addition, the applicability of this reaction is discussed with the extended reaction scope, consisting of 15 substituted phenyl cyclohexenes. Compounds mimicking the functional groups on the carbon surface are utilized as models to study the reaction mechanism and combined with the blocking of specific functional groups on the carbon surface to identify the active sites. Additionally, the effect of acid addition is examined to further investigate the mechanism.

Results

The ODH Reaction. The ODH of phenyl cyclohexene was employed as the standard reaction for the screening of the catalytic activity of carbon materials. The reaction was run in anisole at 140 °C under five bar O_2 for 28 h, according to the previous optimization for analogous oxidative aromatization reactions (28). In the absence of the catalyst, the reaction did not proceed at all, confirming the catalytic role of the added carbon material. AC_{dm} converted 60% phenyl cyclohexene, yielding 22% biphenyl with a 37% selectivity. With oAC_{air} and oAC_{HNO_3} as catalysts, phenyl cyclohexene was completely converted, and the biphenyl yields were up to 74% and 69% with a 74% and 69% selectivity, respectively. *SI Appendix, Fig. S2*, shows the product and by-product distribution in the GC spectra of the crude when the oAC_{air} is the catalyst. The main by-products are an oxidative product and a coupling product with anisole.

The yields of biphenyl obtained with the three catalysts are plotted as a function of the reaction time in Fig. 1A. The experimental data fit well with the exponential function (Eq. 1), (dashed lines in Fig. 1A).

$$C_t = C_0 \exp(-kt), \quad [1]$$

With assumptions: 1) oxygen is more excessive than the reaction demand. 2) The side reactions are ignorable. 3) Internal and external diffusion barriers are ignorable, in the low conversion range, i.e. <6 h, the rate constant is derived with correlation

$$\ln(C_t/C_0) = -kt, \quad [2]$$

where k is the rate constant, C_0 is the phenyl cyclohexene initial concentration, C_t is the phenyl cyclohexene concentration at time t , and t is the reaction time. The quality of the correlation is illustrated in Fig. 1B. The slopes derived are the reaction rate constants with values 8.3×10^{-3} , 9.1×10^{-2} , and $6.3 \times 10^{-2} \text{ h}^{-1}$ for the samples AC_{dm} , oAC_{air} , and oAC_{HNO_3} , respectively.

With the increase of temperature from 100 to 140 °C, the reaction rate constant of oAC_{air} catalyzed ODH reaction increased from $1.6 \times 10^{-2} \text{ h}^{-1}$ to $9.1 \times 10^{-2} \text{ h}^{-1}$, see Fig. 2A. The apparent activation energy of the ODH reaction with sample oAC_{air} as the catalyst follows the Arrhenius law:

$$\ln(k) = \ln(A) - E_a/(RT). \quad [3]$$

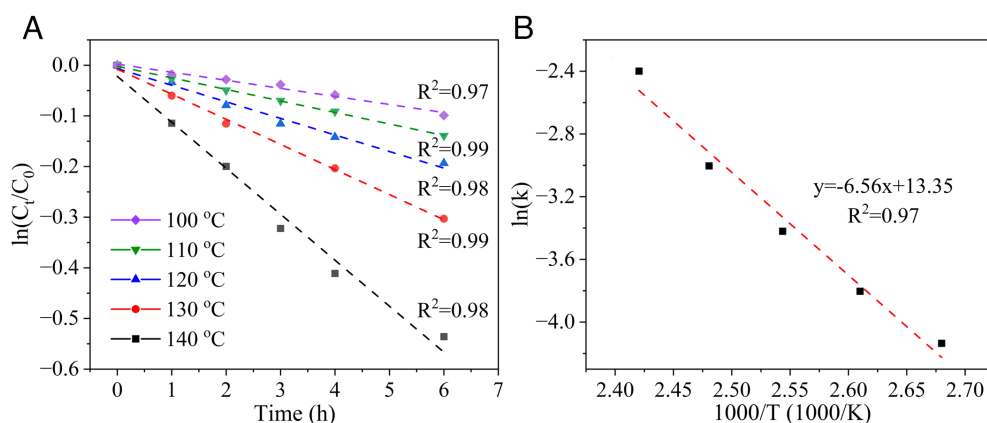


Fig. 2. (A) The relationship between $\ln(C_t/C_0)$ and reaction time with temperature (B) The relationship between $\ln k$ and $1000/T$. The reactions are carried out with the oAC_{air} catalyst under five bar O_2 at different temperatures.

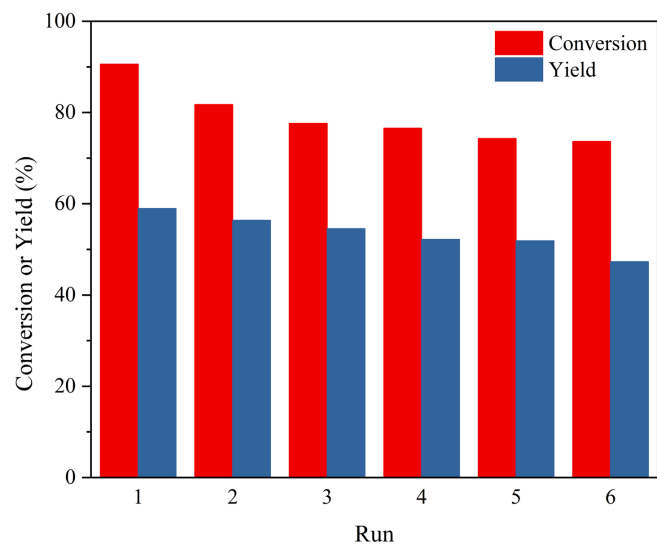


Fig. 3. Catalyst recyclability test over six cycles in anisole with oAC_{air} for 24 h under five bar O_2 at 140°C . The conversion and yield were determined via GC using dodecane as an internal standard.

where k is the rate constant, A is the preexponential constant, E_a is the apparent activation energy, T is the temperature, and R is the gas constant, $8.314\text{ J}\cdot\text{mol}^{-1}\cdot\text{K}^{-1}$. As shown in Fig. 2B, the slope gives the apparent activation energy as $54.5\text{ kJ}\cdot\text{mol}^{-1}$, which is in the range of chemical reaction and an indication that the reaction is intrinsic kinetics controlled.

The oAC_{air} catalyst was reused 6 times, and the yield versus cycling time is presented in Fig. 3. The conversion of phenyl cyclohexene decreases from 91 to 73%, and the biphenyl yield decreases from 58 to 48% after six runs. The kinetic study shows that the reaction rate constant of the oAC_{air} -catalyzed ODH reaction decreased to $4.8 \times 10^{-2}\text{ h}^{-1}$ after six runs (SI Appendix, Fig. S4). Despite the slower conversion rate, the obtained product yield only drops by 10% after six cycles. The recycled catalyst after one reaction cycle was reactivated under N_2 at 450°C for 4 h, but the activity was not recovered, only resulting in a 86% conversion of phenyl cyclohexene and a 53% yield of biphenyl.

Extension of Biaryl ODH Reaction. To examine the applicability of the reaction system and the effect of the substitution groups, the ODH aromatization of phenyl cyclohexene with different substitution groups on both the phenyl and cyclohexene moieties was tested. The results are listed in Table 1. oAC_{air} shows high activity for the ODH of substrates with electron-donating groups (EDG) in *para*- and *meta*-positions (4- and 3-substituted) of the aromatic ring: 4-methoxy-substituted, 4-methoxy-3-methyl-substituted, 4-methoxy-3,5-dimethyl-substituted phenyl cyclohexenes (**1b**, **1c**, and **1d**) were completely converted and produced 4-methoxy biphenyl, 4-methoxy-3-methyl biphenyl, and 4-methoxy-3,5-dimethyl biphenyl (**2b**, **2c**, and **2d**) with yields of 77%, 83%, and 85%, respectively, higher than the yield of biphenyl (**2a**) produced from phenyl cyclohexene (**1a**), and comparably higher selectivities (77%, 83%, and 85%). The presence of an electron-withdrawing group (EWG) in the *meta*-position, instead, lowered the reaction selectivity, as 3-fluoro-4-methoxy-substituted phenyl cyclohexene (**1e**) was almost completely converted, but 3-fluoro-4-methoxy biphenyl (**2e**) was obtained in a 66% yield and a 68% selectivity. The same trend is observed when an EDG is situated in 2-position: 2-methoxy biphenyl (**2f**) was obtained only in a 54% yield and a 55% selectivity from 2-methoxy substituted phenyl cyclohexene

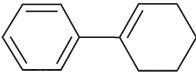
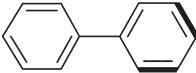
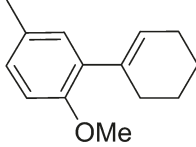
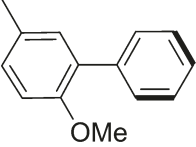
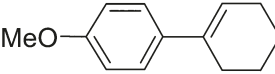
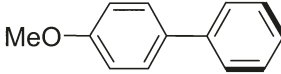
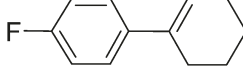
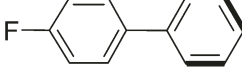
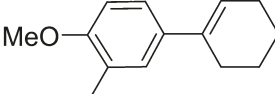
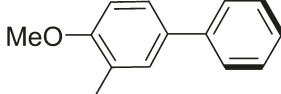
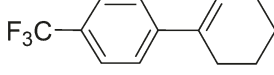
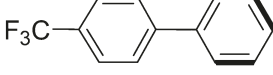
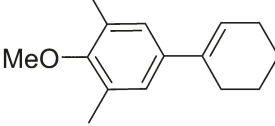
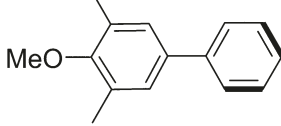
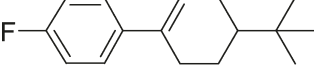
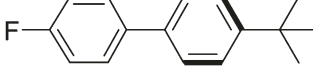
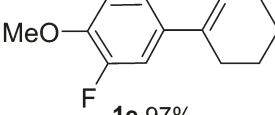
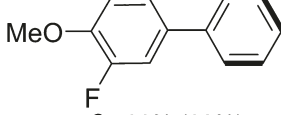
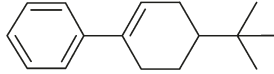
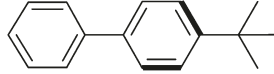
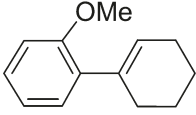
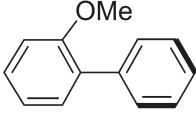
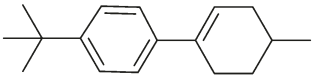
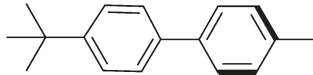
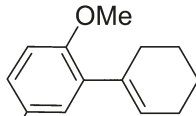
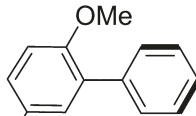
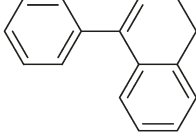
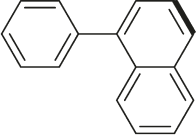
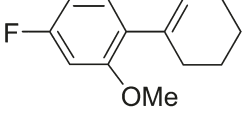
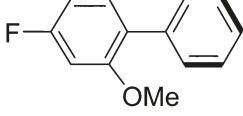
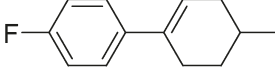
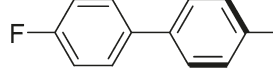
(**1f**) despite being almost completely converted. As expected, the addition of an EWG in the *para*- and *meta*-position further lowered the yield, while an EDG in the *para*-position improved the yield. 5-fluoro-2-methoxy biphenyl, 4-fluoro-2-methoxy biphenyl, and 2-methoxy-5-methyl biphenyl (**2g**, **2h**, and **2i**) were obtained from 5-fluoro-2-methoxy substituted, 4-fluoro-2-methoxy substituted, and 2-methoxy-5-methyl substituted phenyl cyclohexene (**1g**, **1h**, and **1i**) with, respectively, 61%, 74%, and 92% as conversion and 41%, 48%, and 67%, as yields. The reaction proceeds more slowly in the presence of EWG in the *para*-position, 4-fluoro biphenyl and 4-trifluoromethyl biphenyl (**2j** and **2k**) were obtained from 4-fluoro and 4-trifluoromethyl phenyl cyclohexene (**1j** and **1k**) with rather low yields, 28% and 26%, respectively. **1j** and **1k** were converted 88% and 64%, respectively. In contrast, the reaction system tolerates EDG in the 4'-position on the cyclohexene ring (R^1), 4-fluoro-4'-tertbutyl biphenyl, 4'-tertbutyl biphenyl, and 4-tertbutyl-4'-methyl biphenyl (**2l**, **2m**, and **2n**) were obtained from 4-fluoro-4'-tertbutyl, 4'-tertbutyl, and 4-tertbutyl-4'-methyl phenyl cyclohexene (**1l**, **1m**, and **1n**) in good yields, 74%, 65%, and 67%, respectively, and the substrates were almost completely converted. Due to the already partially unsaturated naphthalene ring, 1-phenyl naphthalene (**2o**) was obtained with an 88% yield from the complete consumption of 1-phenyl-3,4-dihydronaphthalene (**1o**). As a valuable and well-known intermediate of the antiapoptotic protein Bcl-xL, 4-fluoro-4'-methyl biphenyl (**2p**) was obtained in 60% yield from 4-fluoro-4'-methyl phenyl cyclohexene (**1p**) at 67% conversion. Beyond the substituted phenyl cyclohexenes, 1-methyl cyclohexene was tested to determine whether alkyl-substituted cyclohexenes could be aromatized as well with this method, resulting in a 24% conversion and a 7% yield of toluene under the above condition.

Hammett plot is a method to describe how the *meta*- or *para*-phenyl substituents influence the activity of the substrates related to reaction rates (31). Different reactions will exhibit different influences which are related to the charging state of intermediates. Hammett plot of 4-substituted phenyl cyclohexene (**1a**, **1b**, **1j**, and **1k**) based on the data in Table 1 is illustrated in Fig. 4A. Linear fitting of the values obtained for substrates with only one substituting group on the phenyl ring shows excellent correlation ($R^2 = 0.985$) between the substituent constant σ_{para} values and the ratio of reaction rate constant with substituent to the rate without substituent $\log(k/k_0)$. The observed negative reaction constant ρ -value (-0.96 , Fig. 4A) indicates the formation of a positively charged intermediate (28).

Catalyst Characterization. The surface area, mean pore diameter, and total pore volume of the catalyst samples used in this work were characterized with a N_2 adsorption technique, and the results are listed in Table 2. All four samples, in which Re- oAC_{air} was the recovered sample after six runs, have type IV adsorption isotherms. Mesopores exist in all the four samples, and the oxidation treatments have a minor influence on the mean pore diameter (3.55 to 3.77 nm) but have a remarkable influence on the surface area. The surface areas measured are 7.56×10^2 , 1.28×10^3 , 6.42×10^2 , and $1.12 \times 10^3\text{ m}^2/\text{g}$ for AC_{dm} , oAC_{air} , $\text{oAC}_{\text{HNO}_3}$, and Re- oAC_{air} samples, respectively. In addition, the total pore volume of the 4 samples follows the same trend, and they are 7.14×10^{-1} , 1.17 , 5.40×10^{-1} , and $1.02\text{ cm}^3/\text{g}$, respectively.

Fig. 5 shows the Fourier transform infrared spectroscopy (FTIR) spectra of the three fresh samples. In the spectrum of AC_{dm} , the weak peaks at $3,250\text{ cm}^{-1}$, $1,725\text{ cm}^{-1}$, and $1,550\text{ cm}^{-1}$ are ascribed to the vibration of $-\text{OH}$, $\text{C}=\text{O}$ in the carboxylic group and $\text{C}=\text{O}$ in the carbonyl group (27, 30), and the strong peaks in the range of $1,150$ to 900 cm^{-1} are assigned to the vibration of

Table 1. Dehydrogenative aromatization of substituted phenyl cyclohexenes

Conversion of substrate	Isolated yield (selectivity)	Conversion of substrate	Isolated yield (selectivity)
 1a 98%	 2a 72% (73%)	 1i 92%	 2i 67% (73%)
 1b 100%	 2b 77% (77%)	 1j 88%	 2j 28% (32%)
 1c 100%	 2c 83% (83%)	 1k 64%	 2k 26% (41%)
 1d 100%	 2d 85% (85%)	 1l 97%	 2l 74% (76%)
 1e 97%	 2e 66% (68%)	 1m 98%	 2m 65% (66%)
 1f 98%	 2f 54% (55%)	 1n 100%	 2n 67% (67%)
 1g 61%	 2g 41% (67%)	 1o 100%	 2o 88% (88%)
 1h 74%	 2h 48% (65%)	 1p 67%	 2p 60% (90%)

C-O in esters and hydroxyl groups (32). In the spectra of oAC_{air} and $\text{oAC}_{\text{HNO}_3}$, the intensities of the peaks for C=O and C-O are obviously strengthened, indicating that the oxidation treatments increase the amount of the oxygenated functional groups of the carbon catalysts.

The O1s XPS spectra of the four samples are shown in Fig. 6. The O1s spectra are deconvoluted into five bands which are attributed to H_2O , O-C=O, C-O esters, C-OH, and C=O, respectively. The total amount of the oxygenated functional group is the sum of the five bands. The total amount of the oxygenated functional groups is 13.1% for AC_{dm} . After oxidation with air and HNO_3 ,

these values are enhanced to 27.2% and 40.0%. After being recycled for six times, this value of oAC_{air} increases to 32.0%. In addition, comparing Fig. 6B with Fig. 6D, the carbonyl content of oAC_{air} decreases from 8.47 to 7.85% after recycling, while the contents of O-C=O, C-O, C-OH, and H_2O increase.

Reaction with Scavengers and Acid. Two radical scavengers, butylated hydroxytoluene (BHT) and 2,2,6,6-tetramethylpiperidin-1-yl oxidanyl (TEMPO), were added to the reactor during the reaction with oAC_{air} as the catalyst, respectively. BHT is often used as an antioxidant for its ability to trap oxygen radicals such

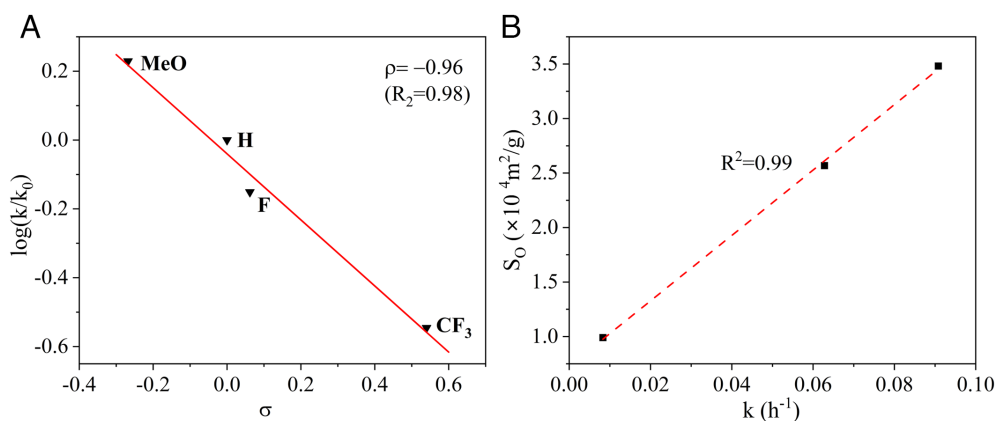


Fig. 4. (A) The Hammett plot for 4-substituted phenyl cyclohexenes (B) The relationship between the reaction rate constant and the effective oxygenated surface area, S_0 .

as superoxide and hydroperoxyl radicals, while TEMPO has been employed for the trapping of both peroxy and benzyl radicals (33, 34). The reaction was slightly slowed down with the addition of both the compounds, as the yields after 6 h (36% and 38%) were slightly lower than the yield without these additives (43%). However, after 28-h reaction, the final conversion showed no obvious difference, and the yields were close for the three reactions. In addition, no radical was trapped by the scavenger. These results indicate that the phenyl cyclohexene ODH reaction does not happen via a free radical pathway.

The methanesulfonic acid addition was tested, and the effect of the acid amount is plotted in Fig. 7A. With 0.015 mmol of the acid, the reaction rate was noticeably higher than that in the test without the acid in the initial stage of the reaction, increasing the yield from 42 to 57% in 6 h. Nevertheless, the final yield achieved the same value as in the test in the absence of the acid, and the substrates were completely converted. With 0.15 mmol of the acid, the final yield at 28 h was lower than that in the test without the acid. Fig. 7B plots the results of the reaction at the beginning of 6 h according to (Eq. 1); the three rate constants are $9.1 \times 10^{-2} \text{ h}^{-1}$, $1.3 \times 10^{-1} \text{ h}^{-1}$, and $9.5 \times 10^{-2} \text{ h}^{-1}$ for the tests with adding 0.0, 1.5×10^{-2} , and 1.5×10^{-1} mmol of the acid, respectively.

Reaction with Blocking Compounds and Catalyst Model Compounds. The C=O, COOH, and C-OH functional groups on oAC_{air} were blocked with phenylhydrazine, benzoic anhydride, and 2-bromoacetophenone, respectively, according to refs. 27 and 35–37. The reactions were carried out at the typical condition (140 °C, five bar O_2 pressure, 3 mL anisole, and 0.01 g catalyst). When C=O groups were blocked, the reaction resulted in significantly decreased activity, conversion decreasing from 98 to 55% and yield decreasing from 71 to 32% at 28 h. However, the blocking of

Table 2. Textural analysis of AC_{dm} , oAC_{air} , $\text{oAC}_{\text{HNO}_3}$, and Re- oAC_{air}

Carbon catalyst	BET surface area (m^2/g)	Mean pore diameter (nm)	Total pore volume (cm^3/g)
AC_{dm}	7.56×10^2	3.77	7.14×10^{-1}
oAC_{air}	1.28×10^3	3.65	1.17
$\text{oAC}_{\text{HNO}_3}$	6.42×10^2	3.55	5.40×10^{-1}
Re- oAC_{air}	1.12×10^3	3.65	1.02

–OH and –COOH groups did not produce considerable activity changes.

The activities of two model compounds, anthraquinone and phenanthrenequinone, of the carbon catalyst were tested at a higher temperature (200 °C), and the results are listed in Table 3. Anthraquinone is a model of ketonic carbonyl groups, but here it exhibited a 38% phenyl cyclohexene conversion and a 2% biphenyl yield. In contrast, phenanthrenequinone, a model for quinoidic carbonyl groups, produced a 35% biphenyl yield at 74% conversion.

Discussion

Applicability and the Extended Scope. Table 4 lists the recent works on ODH reactions of similar molecules, catalyzed by carbon and metal catalysts. Compared to gas-phase ODH reactions, this work carried out the ODH reaction at a lower temperature. Most common gas-phase ODH reactions are carried out at temperatures higher than 400 °C (22, 23, 38), while liquid-phase ODH reactions are carried out at 150 °C (Table 4 entries 1, 3, 4, and 6). In the liquid-phase reactions, oAC_{air} as a heterogeneous catalyst is more efficient than the homogenous TEMPO catalyst (Table 4

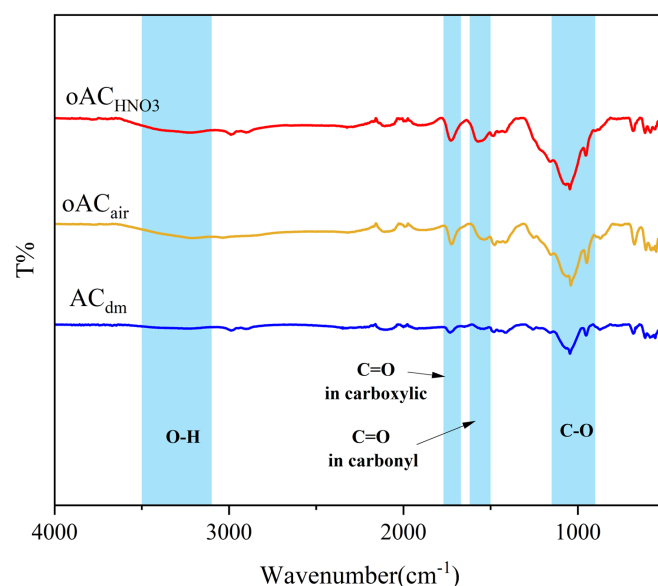


Fig. 5. IR spectra of AC_{dm} , oAC_{air} , and $\text{oAC}_{\text{HNO}_3}$.

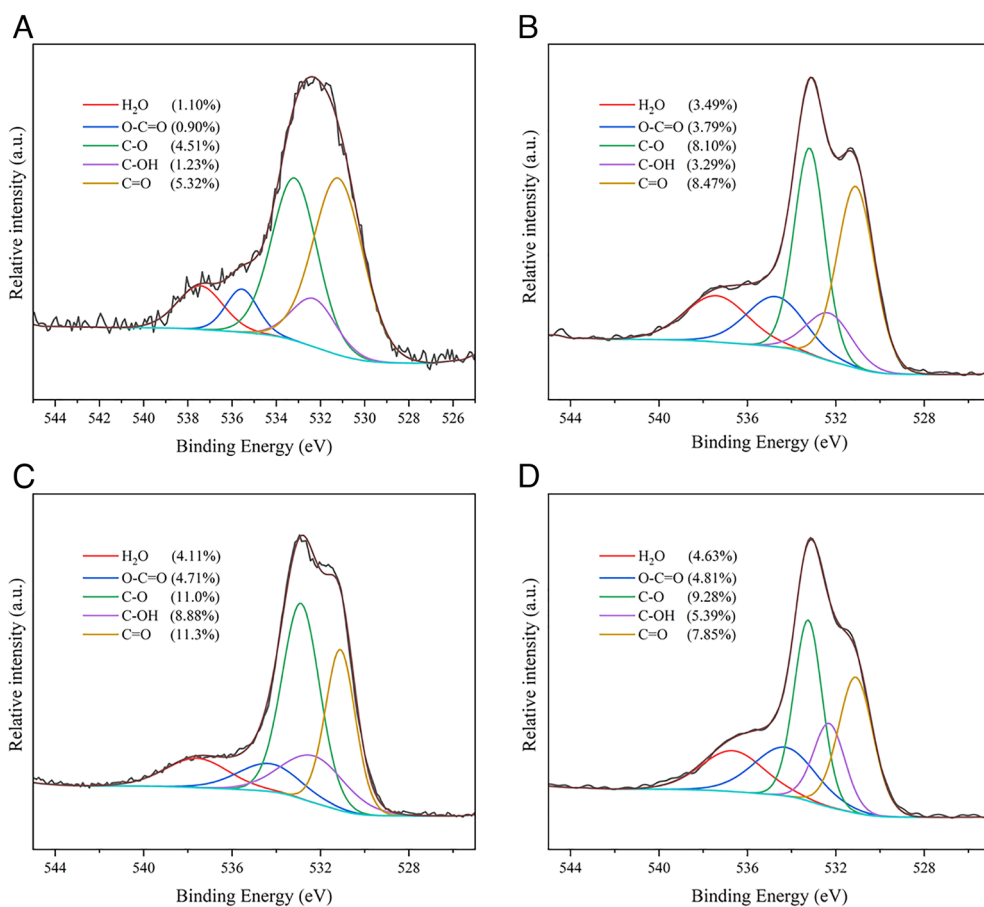


Fig. 6. The O1s XPS spectra of (A) AC_{dmr}, (B) oAC_{air}, (C) oAC_{HNO₃r}, and (D) Re-oAC_{air}. The percentages indicate the percentage of that O atom on the surface of the samples.

entries 2, 5, and 6) (39). Meanwhile, the activity of oAC_{air} in the ODH reaction is comparable with the metal catalyst (Table 4 entries 6 and 7) (17). Therefore, the oAC_{air} is an efficient catalyst for the ODH reaction of aryl cyclohexenes, and it is a metal-free heterogeneous catalyst for this reaction.

To explore the applicability of the ODH route with a carbon catalyst, 15 substituted phenyl cyclohexenes were tested with oAC_{air} as the catalyst, including benzene ring substituted compounds, cyclohexene ring-substituted compounds, and monounsaturated compounds. When the substituted groups were on the

cyclohexene ring (**1l**, **1m**, and **1n**), the targeted product was obtained with a lower yield. When the EDG groups were on the benzene ring, the substituted substrates (**1b**, **1c**, **1d**, and **1f**) were converted with an acceptable yield of targeted products. However, the reactions were in low efficiency when the EWG groups were on the para position of the benzene ring (**1j** and **1k**). To access these substituted biphenyls, introducing additional EDG groups on the benzene ring (**1j** and **1h**) was favorable. In addition, this reaction was applicable to monounsaturated compounds like **1o**. This reaction has the potential to be applied in pharmaceutical

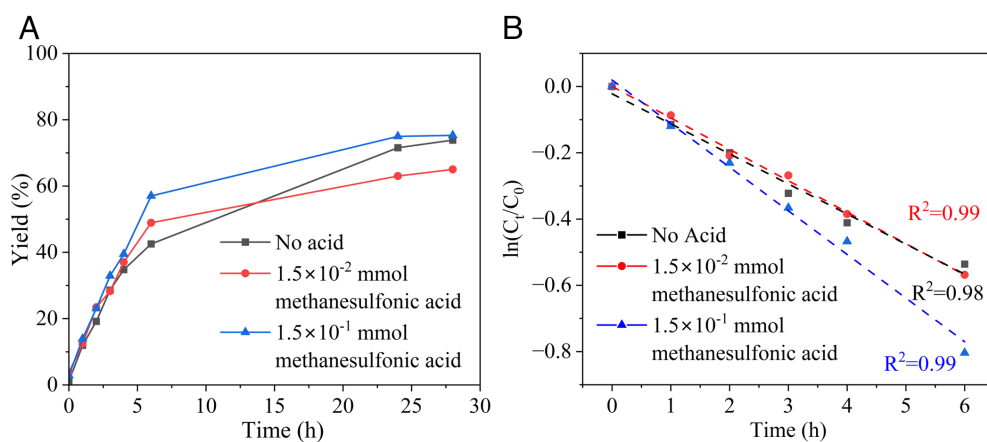
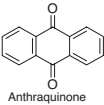
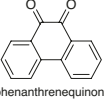


Fig. 7. (A) The yield-reaction time curves with different methanesulfonic acid amounts with oAC_{air} catalysts under five bar O₂ at 140 °C. (B) The relationship between ln(C_t/C₀) and reaction time with different acid amounts.

Table 3. Test of molecular model compounds mimicking the possible active sites of carbon catalysts

Entry	Name of compound	Conversion (%)	Yield (%)
1	No model compound	62	0
2	 Anthraquinone	38	2
3	 phenanthrenequinone	74	35

production as it successfully synthesized product **2p** which can be efficiently converted to 4-fluoro-4'-carbonylic acid-biphenyl, the precursor of the potent inhibitor of the antiapoptotic protein Bcl-xL (40–42).

The Active Site on the Carbon Catalyst. The ODH reaction rate of phenyl cyclohexene fits a first-order kinetics model, and the sample oAC_{air} exhibits the highest activity among the three samples with a reaction rate constant $9.1 \times 10^{-2} \text{ h}^{-1}$. The activity of $\text{oAC}_{\text{HNO}_3}$, with $k = 6.3 \times 10^{-2} \text{ h}^{-1}$, is higher than that of the sample AC_{dm} , here $k = 8.3 \times 10^{-3} \text{ h}^{-1}$. This means that the oxidation treatment is an effective way to enhance the activity toward ODH reactions. The FT-IR spectra show that surface oxygenated functional groups are introduced by the oxidation treatment. Comparing the XPS and Brunauer–Emmett–Teller (BET) results of the oxidized carbon catalysts with the original AC_{dm} , the high activity of $\text{oAC}_{\text{HNO}_3}$ is ascribed to the remarkable amount of oxygenated functional groups (40.0%), while the high activity of oAC_{air} is ascribed to both the notable amount of oxygenated functional groups (27.2%) and high specific surface area $1.28 \times 10^3 \text{ m}^2/\text{g}$. Here, the overall effective oxygenated surface area, i.e., S_{O} , is defined as the surface area multiplied by the total amount of the oxygenated functional groups. The plotting of the reaction rate constant against the effective oxygenated surface area gives a straight line as shown in Fig. 4B.

In the previously investigated ODH reactions with substrates such as ethylbenzenes (11, 27, 30), cyclohexanol, alkanes, and N-heterocycles, the quinoidic carbonyl group has been proposed as the active site of carbon catalysts in the ODH reactions. Here, the quinoidic groups are proven to be the active site in the ODH reaction of phenyl cyclohexene again with the functional group blocking experiments and model compound experiments. The

functional group blocking experiment results show that the carbonyl content has a direct relationship with the ODH reaction activity. The reaction with the quinoidic model compound, phenanthrenequinone, achieved a 35% yield of biphenyl, while only a 2.0% yield of biphenyl was obtained with the ketonic model compound, anthraquinone. These results are consistent with the previous conclusion that the quinoidic carbonyl group on the carbon catalyst surface is the active site of the ODH reaction of other alkanes (43–45).

In the recycling experiment, the yield of biphenyl with oAC_{air} slightly decreased by 10% after six runs. Meanwhile, based on the deconvolution of the O1s spectra of oAC_{air} and $\text{Re-oAC}_{\text{air}}$ (Fig. 6 B and D), the amount of carbonyl groups decreases, but the amount of other oxygenated functional groups increases. This result further proves that it is the carbonyl group rather than other oxygenated functional groups that directly contribute to the activity of carbon catalysts.

Reaction Mechanism. In the experiments with scavengers, no radical was observed, indicating that this reaction does not follow the free-radical-induced reaction process. The decrease in the reaction rate in the first stage of the reaction in the presence of scavengers can be ascribed to the consumption of oxygen by said scavengers, which inhibits the reactivation of the carbonylic active sites (33, 46).

The addition of a small amount of acid ($1.5 \times 10^{-2} \text{ mmol}$ methanesulfonic acid) clearly accelerates the reaction to $1.3 \times 10^{-1} \text{ h}^{-1}$. As previously reported, the addition of acid improves the hydrogen abstraction activity of carbonyl groups and makes the active sites easy to reoxidize (47, 48). This supports the hypothesis that the redox cycle of the quinoidic compound is involved in the ODH reaction. In addition, the substituted group on the cyclohexene ring has little influence on the ODH reaction activity, while the substituted group on the benzene ring influences the reaction activity. This indicates that the ODH reaction experiences a charged intermediate stage which is affected by the inductive effect of the substituted group on the benzene ring. The negative Hammett plot slope ($\rho = -0.96$) indicates that the positively charged intermediate exists in the first step. According to the stability of the benzylic cation and the symmetry, the structure and charge distribution of the positively charged intermediate are proposed in Scheme 1.

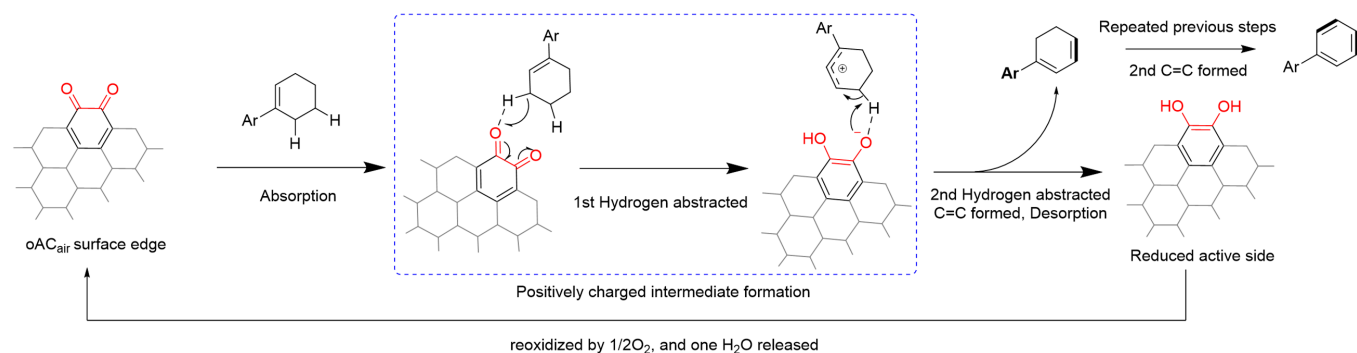
Therefore, the mechanism of the phenyl cyclohexene ODH reaction is based on the redox cycle of the quinoidic carbonyl group as shown in Scheme 1. In the 1st step, the phenyl cyclohexene is absorbed by the quinoidic active site. Then, the one hydrogen in the cyclohexene ring is abstracted by the quinoidic carbonyl group, and

Table 4. Varieties of ODH reaction catalyzed by metal or carbon catalysts

Entry	Substrate	Temperature	Pressure	Catalyst	Reaction		Reference
					time	Yield/ selectivity(%) [*]	
1 [†]	Ethylbenzene	550 °C	C ₈ H ₁₀ /Ar flow	N-AC	-	95	(22)
2	Ethylbenzene	125 °C	air	TEMPO	72 h	25	(36)
3 [†]	Ethane	400 °C	C ₂ H ₆ /O ₂ /He flow	MCNT	-	70	(23)
4 [†]	Propane	550 °C	C ₃ H ₈ /He flow	Nanodiamonds	-	90	(35)
5	Phenyl cyclohexene	130 °C	air	TEMPO	72 h	50	(36)
6	Phenyl cyclohexene	140 °C	5 bar O ₂	oAC_{air}	28 h	74	This work
7	Phenyl cyclohexene	80 °C	air	Cu ⁰ /Selectfluor	24 h	90	(17)

^{*}Selectivity for gas phase reaction.

[†]Reactions are carried in gas phase.



Scheme 1. Proposed mechanism for the ODH reaction of phenyl cyclohexene.

the positively charged intermediate forms. In the 3rd step, the second hydrogen is abstracted, and the quinoidic carbonyl group is reduced to hydroxyl groups. The C-C double bond forms, and the molecule is desorbed from the active site. This molecule experiences the same process and the biphenyl forms. Meanwhile, to complete the redox cycle, the hydroxyl groups (reduced active site) are reoxidized to quinoidic carbonyl groups by oxygen, and one molecular water is released. This mechanism is consistent with the other literature reported ODH reactions catalyzed by carbon catalysts.

Conclusions

A metal-free route with an oxidized activated carbon, oAC_{air} , catalyzed ODH reaction has been developed to synthesize biaryls. The utilized metal-free carbon material operates in a catalytic fashion using O_2 as the terminal oxidant. The developed oAC material offers improved efficiency, compared to other reported carbon allotropes like carbon nanotubes and graphite. The high activity of oAC_{air} is illustrated by the kinetic study where it exhibits the highest reaction rate constant ($k = 9.1 \times 10^{-2} \text{ h}^{-1}$). We report the apparent activation energy of ODH reaction catalyzed with oAC_{air} , which is $54.5 \text{ kJ} \cdot \text{mol}^{-1}$. The catalytic behavior and robustness of the oAC_{air} was confirmed by recyclability tests, which showed remarkable stability over six cycles. The quinoidic active site and the quinoidic redox cycle mechanism are proved via XPS, functional group blocking experiments, and model compound experiments, which is consistent with carbon-catalyzed ODH of other substrates. Hammett plot suggests a positively charged intermediate, and the structure of this intermediate is proposed. The promoting effect of acid (methanesulfonic acid) toward the reaction is confirmed.

The devised alternative route to biaryls opens a path for the synthesis of a family of biaryl-containing medical compounds in the liquid phase, traditionally relying on highly toxic chemicals as well as transition metal catalysts. The extended reaction scope consisting of 15 differently substituted aryl cyclohexenes has proven the wide applicability of this ODH reaction. We expect that this work will pave the way for further development of carbon-based catalysts for ODH reactions to offer robust alternatives for transition metal-mediated reactions.

Materials and Methods

Materials. Solvents (AR), including methanol, ethyl acetate, hexane, anisole, and dichloromethane (DCM), and the reagents, such as phenyl cyclohexene (>95%), anthraquinone, phenyl hydrazine, 2-bromo-1-phenyl ethanone, benzoic anhydride, BHT, TEMPO, methanesulfonic acid, and dodecane (>99%), were all purchased from Sigma-Aldrich. The reactant, 4-methoxy-substituted phenyl

cyclohexene, in the reaction scope was prepared with the literature method, and other reactants were prepared with similar method (49).

Preparation of the Catalyst. 8.0 g AC (1 kg batch (lot. H2430) from Fluka with 100 mesh particle size) and 65 mL 1 M HCl were added to a flask, and the mixture was stirred for 6 h at 70 °C. After that, the carbon was filtrated and washed with deionized water and dried in a vacuum oven at 140 °C for 16 h. The material obtained was demetallized and was denoted as AC_{dm} . 4.0 g AC_{dm} was heated to 425 °C for 16 h in air and then heated to 450 °C in Ar for 24 h to obtain the air-oxidized AC (oAC_{air}). Nitric acid-oxidized AC ($\text{oAC}_{\text{HNO}_3}$) was prepared via oxidation of 4.0 g AC_{dm} with 8 mL nitric acid (68% aqueous) at 140 °C for 15 h. The carbon filtrated out was washed and dried in a vacuum oven at 140 °C for 2 h.

Blocking of Functional Groups on Carbon. The procedure was carried out in a 50-mL glass tube under Ar according to the literature (27, 35–37). Phenyl hydrazine was used for blocking C=O on oAC_{air} . Phenyl hydrazine (1.37 mL, 13.9 mmol) and 0.08 mL HCl 12 M were dissolved in 75 mL DCM, and then, oAC_{air} (744 mg) was added. The slurry was stirred at ambient temperature for 72 h. After that, the solid obtained was filtrated and washed with CHCl_3 and DCM sequentially and finally dried under vacuum at 60 °C for 24 h. For the blocking of COOH and OH surface groups, 2-bromo-1-phenyl ethanone and benzoic anhydride were employed, respectively, in a similar procedure.

Catalyst Characterization. A Kratos AXIS Ultra DLD XPS, using a monochromated $\text{Al}_{K\alpha}$ X-ray source (1486.7 eV) running at 100 W, was employed to acquire the XPS spectra. A pass energy of 80 eV and a step size of 1.0 eV were used for the survey spectra, while a pass energy of 20 eV and a step size of 0.1 eV were set for the high-resolution spectra. Photoelectrons were collected at a 90° take-off angle under ultrahigh vacuum conditions, with a base pressure typically below 1×10^{-9} Torr. The diameter of the beam spot of the X-ray was 1 mm, and the area of analysis for these measurements was $300 \mu\text{m} \times 700 \mu\text{m}$. Both survey and high-resolution spectra were collected from three different spots on each sample surface to check for homogeneity and surface charge effects. The total amount of oxygenated groups is the ratio of the peak area of O1s to the peak areas of O1s and C1s.

Nitrogen adsorption/desorption experiments were performed with a TriStar 3,020 instrument at -196 °C. The specific surface area of each sample was calculated by the multiple points BET method. Before measurement, the samples were degassed under a vacuum condition at 120 °C overnight. The FTIR analysis was carried out with PerkinElmer UATR Diamond accessory with two polymer QA/QC analysis systems. The spectra were recorded from 500 cm^{-1} to $4,000 \text{ cm}^{-1}$ wavenumbers with 16 scans.

The Catalytic Reaction. All the reactions were carried out in a 5-mL glass reactor equipped with a pressure gauge and a gas charging and sampling system. In a typical reaction, 0.15 mmol phenyl cyclohexene, 3 mL anisole, 15 mg dodecane (as an internal standard), and 50 to 150 mg catalyst were added into the reactor. The slurry was stirred at 600 rpm/min and heated at 100 to 140 °C for 6 to 28 h under O_2 with different pressure. During the reaction, 0.05 mL sample was taken out from the reactor at 0 h, 1 h, 2 h, 3 h, 4 h, 6 h, 24 h, and 28 h and analyzed with a gas chromatograph (GC). After

the reaction, the catalyst was separated via filtration and washed with DCM (3 × 50 mL). The solvent in products was removed with vacuum evaporation at 40 °C under 10 kPa absolute pressure, and the pure product was obtained with flash chromatography (hexane: ethyl acetate 400:1).

The product was quantitatively analyzed with an Agilent 7,890 GC equipped with a flame ionization detector and qualitatively analyzed with a Shimadzu GC equipped with a mass spectrometer as the detector (GC-MS). The HP-5 capillary column (30 m × 0.32 mm × 0.25 μm, Agilent) and a split ratio of 10 were used for both GCs. The oven temperature program was set from 60 to 300 °C at 15 °C/min and then held at 300 °C for 10 min.

1. I. Cepanec, *Synthesis of Biaryls* (Elsevier, 2010).
2. L. Yet, *Privileged Structures in Drug Discovery: Medicinal Chemistry and Synthesis* (John Wiley & Sons, 2018).
3. Y.-F. Zhang, Z.-J. Shi, Upgrading cross-coupling reactions for biaryl syntheses. *Acc. Chem. Res.* **52**, 161–169 (2019).
4. C. C. Johansson Seechurn, M. O. Kitching, T. J. Colacot, V. Snieckus, Palladium-catalyzed cross-coupling: A historical contextual perspective to the 2010 nobel prize. *Angew. Chem. Int. Ed.* **51**, 5062–5085 (2012).
5. S. Yuan, J. Chang, B. Yu, Construction of biologically important biaryl scaffolds through direct C-H bond activation: Advances and prospects. *Top. Curr. Chem.* **378**, 1–70 (2020).
6. C.-L. Sun, Z.-J. Shi, Transition-metal-free coupling reactions. *Chem. Rev.* **114**, 9219–9280 (2014).
7. F. Zhou, M.-O. Simon, C.-J. Li, Transition-metal-free one-pot synthesis of biaryls from grignard reagents and substituted cyclohexanones. *Chem. Eur. J.* **19**, 7151–7155 (2013).
8. V. Domingo *et al.*, Iodine-promoted metal-free aromatization: synthesis of biaryls, oligo p-phenylenes and a-ring modified steroids. *Adv. Synth. Catal.* **357**, 3359–3364 (2015).
9. Y. Jia *et al.*, Promoted effect of zinc-nickel bimetallic oxides supported on HZSM-5 catalysts in aromatization of methanol. *J. Energy Chem.* **26**, 540–548 (2017).
10. X. Dai *et al.*, Aromatization of hydrocarbons by oxidative dehydrogenation catalyzed by nickel porphyrin with molecular oxygen. *Catal. Commun.* **117**, 85–89 (2018).
11. X. Liu, J. Chen, T. Ma, Catalytic dehydrogenative aromatization of cyclohexanones and cyclohexenones. *Org. Biomol. Chem.* **16**, 8662–8676 (2018).
12. K. Kikushima, Y. Nishina, Copper-catalyzed oxidative aromatization of 2-cyclohexen-1-ones to phenols in the presence of catalytic hydrogen bromide under molecular oxygen. *RSC Adv.* **3**, 20150–20156 (2013).
13. K. Koike, S. Ueno, Palladium-catalyzed dehydrogenative [3+3] aromatization of propyl ketones and allyl carbonates. *Chem. Lett.* **51**, 489–492 (2022).
14. T. Ichikawa *et al.*, Microwave-mediated site-selective heating of spherical-carbon-bead-supported platinum for the continuous, efficient catalytic dehydrogenative aromatization of saturated cyclic hydrocarbons. *ACS Sustainable Chem. Eng.* **7**, 3052–3061 (2019).
15. L. M. Pastrana-Martínez, S. Morales-Torres, F. J. Maldonado-Hódar, A Comparative study of aromatization catalysts: The advantage of hybrid oxy/carbides and platinum-catalysts based on carbon gels. *J. Carbon Res.* **7**, 21 (2021).
16. G. Martra, F. Arena, S. Coluccia, F. Frusteri, A. Parmaliana, Factors controlling the selectivity of V2O5 supported catalysts in the oxidative dehydrogenation of propane. *Catal. Today* **63**, 197–207 (2000).
17. S. Ren *et al.*, Copper/selectfluor-system-catalyzed dehydration-oxidation of tertiary cycloalcohols: Access to β-substituted cyclohex-2-enones, 4-arylcoumarins, and biaryls. *Eur. J. Org. Chem.* **2015**, 5381–5388 (2015).
18. A. Lenarda, T. Wirtanen, J. Helaja, Carbon materials as catalytic tools for oxidative dehydrogenations and couplings in liquid phase. *Synthesis* **55**, 45–61 (2023).
19. J. Zhang *et al.*, Nanocarbon as robust catalyst: Mechanistic insight into carbon-mediated catalysis. *Angew. Chem. Int. Ed.* **46**, 7319–7323 (2007).
20. M. F. R. Pereira, J. J. Órfão, J. L. Figueiredo, Oxidative dehydrogenation of ethylbenzene on activated carbon fibers. *Carbon* **40**, 2393–2401 (2002).
21. J. L. Figueiredo, M. F. R. Pereira, *Carbon as Catalyst* (Wiley Hoboken, NJ, USA, 2009).
22. B. Frank, M. Morassutto, R. Schomäcker, R. Schlögl, D. S. Su, Oxidative dehydrogenation of ethane over multiwalled carbon nanotubes. *ChemCatChem* **2**, 644–648 (2010).
23. R. Wang, X. Sun, B. Zhang, X. Sun, D. Su, Hybrid nanocarbon as a catalyst for direct dehydrogenation of propane: Formation of an active and selective core-shell sp²/sp³ nanocomposite structure. *Chem. Eur. J.* **20**, 6324–6331 (2014).
24. B. Frank, J. Zhang, R. Blume, R. Schlögl, D. S. Su, Heteroatoms increase the selectivity in oxidative dehydrogenation reactions on nanocarbons. *Angew. Chem. Int. Ed.* **48**, 6913–6917 (2009).
25. J. Zhang *et al.*, Surface-modified carbon nanotubes catalyze oxidative dehydrogenation of n-butane. *Science* **322**, 73–77 (2008).
26. I. Pelech, O. S. G. P. Soares, M. F. R. Pereira, J. L. Figueiredo, Oxidative dehydrogenation of isobutane on carbon xerogel catalysts. *Catal. Today* **249**, 176–183 (2015).
27. W. Qi *et al.*, Oxidative dehydrogenation on nanocarbon: Identification and quantification of active sites by chemical titration. *Angew. Chem. Int. Ed.* **52**, 14224–14228 (2013).
28. L. Enders *et al.*, Air oxidized activated carbon catalyst for aerobic oxidative aromatizations of N-heterocycles. *Catal. Sci. Technol.* **11**, 5962–5972 (2021).
29. A. Mollar-Cuni, D. Ventura-Espinosa, S. Martín, H. García, J. A. Mata, Reduced graphene oxides as carbocatalysts in acceptorless dehydrogenation of N-heterocycles. *ACS Catal.* **11**, 14688–14693 (2021).
30. W. Qi, P. Yan, D. S. Su, Oxidative dehydrogenation on nanocarbon: Insights into the reaction mechanism and kinetics via in situ experimental methods. *Acc. Chem. Res.* **51**, 640–648 (2018).
31. E. V. Anslyn, D. A. Dougherty, *Modern Physical Organic Chemistry* (University Science Books, 2006).
32. V. Gomez-Serrano, J. Pastor-Villegas, A. Perez-Florindo, C. Duran-Valle, C. Valenzuela-Calahorra, FT-IR study of rockrose and of char and activated carbon. *J. Anal. Appl. Pyrolysis* **36**, 71–80 (1996).
33. W. A. Yehye *et al.*, Understanding the chemistry behind the antioxidant activities of butylated hydroxytoluene (BHT): A review. *Eur. J. Med. Chem.* **101**, 295–312 (2015).
34. D. H. R. Barton, V. N. Le Gloahec, J. Smith, Study of a new reaction: Trapping of peroxy radicals by TEMPO. *Tetrahedron Lett.* **39**, 7483–7486 (1998).
35. C. Larabi, E. A. Quadrelli, Titration of Zr3(μ-OH) hydroxy groups at the cornerstones of bulk MOF UiO-67, [Zr6O4(OH)4(biphenyldicarboxylate)6], and their reaction with [AuMe(PMe3)]. *Eur. J. Inorg. Chem.* **2012**, 3014–3022 (2012).
36. K. A. Wepasnick *et al.*, Surface and structural characterization of multi-walled carbon nanotubes following different oxidative treatments. *Carbon* **49**, 24–36 (2011).
37. A. Setyan, J. J. Sauvain, M. J. Rossi, The use of heterogeneous chemistry for the characterization of functional groups at the gas/particle interface of soot and TiO₂ nanoparticles. *Phys. Chem. Chemical Phys.* **11**, 6205–6217 (2009).
38. Z. Zhao, Y. Dai, G. Ge, Nitrogen-doped nanotubes-decorated activated carbon-based hybrid nanoarchitecture as a superior catalyst for direct dehydrogenation. *Catal. Sci. Technol.* **5**, 1548–1557 (2015).
39. T. Ito, F. W. Seidel, X. Jin, K. Nozaki, TEMPO as a hydrogen atom transfer catalyst for aerobic dehydrogenation of activated alkanes to alkenes. *J. Org. Chem.* **87**, 12733–12740 (2022).
40. T. V. Bright *et al.*, A convenient chemical-microbial method for developing fluorinated pharmaceuticals. *Org. Biomol. Chem.* **11**, 1135–1142 (2013).
41. A. M. Petros *et al.*, Discovery of a potent inhibitor of the antiapoptotic protein Bcl-xL from NMR and parallel synthesis. *J. Med. Chem.* **49**, 656–663 (2006).
42. M. Li, D. Wang, J. He, L. Chen, H. Li, Bcl-XL: A multifunctional anti-apoptotic protein. *Pharmacol. Res.* **151**, 104547 (2020).
43. Y. Kawashita, N. Nakamichi, H. Kawabata, M. Hayashi, Direct and practical synthesis of 2-arylbenzoxazoles promoted by activated carbon. *Org. Lett.* **5**, 3713–3715 (2003).
44. J. L. Figueiredo, M. F. R. Pereira, M. M. A. Freitas, J. J. M. Órfão, Modification of the surface chemistry of activated carbons. *Carbon* **37**, 1379–1389 (1999).
45. A. Brunmark, E. Cadenas, Redox and addition chemistry of quinoid compounds and its biological implications. *Free Radical Biol. Med.* **7**, 435–477 (1989).
46. Y.-Q. Huang, H.-J. Song, Y.-X. Liu, Q.-M. Wang, Dehydrogenation of N-heterocycles by superoxide ion generated through single-electron transfer. *Chem. Eur. J.* **24**, 2065–2069 (2018).
47. X. Liu *et al.*, Manganese dioxide-methanesulfonic acid promoted direct dehydrogenative alkylation of sp³ C-H bonds adjacent to a heteroatom. *J. Org. Chem.* **78**, 3104–3112 (2013).
48. E. Sheikhi, M. Adib, M. A. Karajabad, S. J. A. Gohari, Sulfuric Acid-promoted oxidation of benzylic alcohols to aromatic aldehydes in dimethyl sulfoxide: An efficient metal-free oxidation approach. *Synlett* **29**, 974–978 (2018).
49. L. Li, G. Hilt, Regioselective DH or HD addition to alkenes: Deuterohydrogenation versus hydrodeuterogenation. *Org. Lett.* **22**, 1628–1632 (2020).

Data, Materials, and Software Availability. All study data are included in the article and/or *SI Appendix*.

ACKNOWLEDGMENTS. We are grateful to Jane ja Aatos Erkon Säätiö (Jane and Aatos Erkkö Foundation) for the financial support to “BioCat” project (J.H. & Y.L.).

Author affiliations: ^aDepartment of Chemical and Metallurgical Engineering, School of Chemical Engineering, Aalto University, Espoo 02150, Finland; and ^bDepartment of Chemistry, University of Helsinki, Helsinki 00014, Finland